

Nuclear to quark-matter transition in the string-flip model

C. J. Horowitz

Nuclear Theory Center and Department of Physics, Indiana University, Bloomington, Indiana 47405

J. Piekarewicz

Supercomputer Computations Research Institute, Florida State University, Tallahassee, Florida 32306

(Received 20 May 1991)

We have calculated ground-state properties of nuclear matter in a simple string-flip quark model in one dimension. Special emphasis was placed on the transition from hadron to quark matter and to the response of the system to color fields. Numerical simulations involving a large number of quarks were carried out for two- and three-quark clusters. This in turn enabled us to investigate the hadron-to-quark transition through the study of finite-size effects. The concept of a sudden-quark potential was introduced as an example of a generic response of the medium to color fields. We have argued that this response might be relevant to the propagation of a rapidly moving quark-antiquark pair (e.g., J/ψ meson) through the medium.

I. INTRODUCTION

One of the main thrusts behind the newly commissioned nuclear physics facilities (CEBAF, RHIC) is the possibility of unambiguously identifying quark signatures in nuclei. Unfortunately, quark signatures in nuclear phenomena have, so far, proved elusive. Much of the success of these facilities will therefore rely on strong theoretical programs that will search for and identify areas sensitive to the quark substructure of nucleons. One of the objections most often raised by the critics of conventional nuclear structure models is that, because of the intrinsic size of the objects, a picture of nucleons interacting in the medium via meson exchanges is inappropriate. The process is claimed to resemble three highly overlapping quark bags where the identification of nucleons and mesons is ambiguous at best. Still, there seems to be ample experimental evidence that will support that, although some properties of the nucleon may be modified inside the nuclear medium, a nucleon inside the nucleus resembles to a very good approximation a nucleon in free space. Furthermore, to date, there is no compelling evidence that will even indicate that some of these medium modifications are beyond conventional explanations. Perhaps the greatest challenge facing nuclear physics today is the explanation of these remarkable facts, namely, how can such successful hadronic models emerge from the basic underlying theory with quarks and gluons as fundamental degrees of freedom.

It is also interesting to note that, although most of these questions have been posed since the advent of QCD, remarkably little progress has been made in answering them. A serious difficulty encountered when attempting to answer these questions is how to model a system that is believed to have quarks confined inside hadrons at low density while free quarks at high density. Most calculations that attempt to address the quark substructure of

nucleons have then resorted to phenomenological descriptions. In some of these approaches, for example, one introduces *ad hoc* parameters to determine the transition from a hadron-based to a quark-based description of the process. To date, however, there are very few calculations of uniform quark matter that attempt to reproduce nuclear-matter properties using exclusively quark degrees of freedom [1,2,3]. A particular version of these, the so-called string-flip model, will be used throughout this work.

In the string-flip model quarks interact via a truly many-body potential. The many-body nature of the potential allows quarks to be confined inside hadrons, but at the same time enables the force to saturate; i.e., hadrons can separate without generating strong van der Waals forces (cluster separability). Furthermore, quarks are treated as identical particles and all processes are described in terms of an explicitly antisymmetric quark wave function. Another virtue of the model is that the dynamics, given entirely in terms of a quark-confining potential and exchange symmetry, generates the following limits: a hadron gas at low density and a quark Fermi gas at high density. The model, however, has serious limitations. The string-flip model is intrinsically nonrelativistic and, as such, does not satisfy fundamental symmetry principles of QCD, like chiral symmetry and Lorentz invariance. Nevertheless, nonrelativistic constituent quark models have proved to be very useful in the understanding of hadron spectroscopy and hadronic resonances [4]. It is in this spirit that we use this model.

In this and future work we want to use the string-flip model to address a variety of issues. Initially, one would like to understand ground-state properties of quark matter. For example, how do properties of hadrons get modified inside the medium. How much, if any, does the interaction between quarks in the medium get modified because of screening effects. How are well-known prop-

erties of the nucleon-nucleon force (e.g., the strong short-range repulsion) realized in the model. Furthermore, because in the string-flip model the system is known to behave as a hadron gas at low density and a quark Fermi gas at high density, one can also study this hadron-to-quark transition as a function of density. In fact, understanding this transition is the main goal of this work. We want to use the string-flip model to gain some insight into the nature of the transition. We would like to identify, for example, physical observables that may characterize the transition.

There has already been substantial progress made in calculating nuclear-matter observables within the string-flip model [1,2,3]. Among the observables calculated in the past were the energy per quark and length scale for quark confinement as a function of density. Unfortunately, because of limitations in computer power, these observables were only calculated with a small number of quarks ($n \leq 16$). In contrast, numerical simulations involving a large number of quarks might be able to give precise estimates of the importance of finite-size effects. Clearly, the numerical value of any physical observable calculated in infinite quark matter should not depend separately on the number of quarks and the volume of the system. Instead, all observables should only depend on a single intensive variable, namely, the density of the system. In practice, however, numerical simulations are always carried on in a finite-size box with a finite number of quarks. It is therefore important to investigate the sensitivity of physical observables to finite-size effects. More interesting, however, the study of finite-size effects might signal the onset of very exciting phenomena. In particular, at the critical point for a transition, certain correlation lengths become infinite. Consequently, the measurement of these observables on a finite lattice will always show evidence for large finite-size effects. In this work we will carry out simulations involving a large number of quarks (up to 128) in the hope of elucidating details of the hadron-to-quark transition through the sensitivity of some observables to finite-size effects.

We would also like to study the response of the system to color fields. There are a variety of issues that one could in principle address. For example, one would like to study the dielectric properties of the medium and its effectiveness in screening color charge. These issues are of direct relevance to questions of current interest. Understanding the polarizability of the medium, for example, might be of relevance to the formation and propagation of a J/ψ meson in the nuclear medium. In fact, J/ψ suppression in the medium has been advocated by many as one of the clearest signatures for the formation of a quark-gluon plasma in relativistic heavy-ion collisions [5]. In those models the basic mechanism for J/ψ suppression is color screening. The screening of the color force by the medium weakens the interaction between the $c\bar{c}$ pair and, in turn, precludes the formation of the bound state. Another issue that has generated much excitement is color transparency [6,7]. Underlying this idea is the fact that if the color constituents of a rapidly moving hadron are close together (after a hard-scattering process), then the interaction of this “small” hadron with the

medium should be small. One would therefore like to have a model to investigate how a rapidly moving $c\bar{c}$ pair propagates through the medium. Relevant to the above ideas, then, is the study of the response of the system to the sudden introduction of two rapidly moving color charges. In particular, how is the color interaction between this “fast” pair of quarks modified in the medium. We labeled these quarks as fast because we will assume that their rapid propagation through the medium will not affect the dynamics of the “slow” quarks in the system. In particular, the slow-quark dynamics will still be described by the same ground-state wave function, independent of the presence of the two extra quarks. In this work we will use the concept of a sudden-quark potential as an example of a generic response of the medium to color fields. To fully understand the response, however, one is forced to calculate the complete excitation spectrum of the system. This takes us to the second phase of the program.

In future work we will try to examine the different modes of excitation of the system. Particularly interesting will be the search for new modes of excitations not seen in isolated hadrons or present in conventional descriptions of nuclei. Some of these modes might originate from the collective response of many quarks. These “quark giant resonances” may involve coherent density, spin, flavor, and/or color excitations. It will also be interesting to examine the density dependence of collective modes. For example, in the low-density (hadronic) phase, there is a well-known low-energy ($\omega \sim 20$ MeV) spin-isospin mode: the Gamow-Teller resonance. At higher excitation energies ($\omega \sim 300$ MeV), there is also a well-known excitation in the quark degrees of freedom, namely, the nucleon-to-delta ($N \rightarrow \Delta$) transition. It is unknown, however, how the excitation energy, collectivity, and mixing of these hadronlike and quarklike modes will change with density. Presumably, there should be a softening of the $N \rightarrow \Delta$ excitation as one moves away from the low-density phase, where confinement scales dominate, and into the high-density deconfined phase. Hopefully, careful study of these ideas might help elucidate some recent experimental findings that have reported a large (~ 50 MeV) downward shift in the position of the Δ peak measured in several nuclei relative to that on a free proton [8].

The paper is organized as follows. In Sec. II we introduce and review some properties of the string-flip model with particular emphasis on the two-quark ($2Q$) nucleon case in one dimension. We present the main ideas of quark pairing and introduce the one-parameter variational wave function. In Sec. III we generalize the formalism to the three-quark ($3Q$) nucleon case. We should mention that only in one dimension does there exist an efficient algorithm (i.e., nonfactorial) for treating the three-quark nucleon problem. In Sec. IV we present the results of the numerical simulations in one dimension. Some of these results have already been calculated in the past. We include these for completeness. In addition, we present results of simulations involving a large number of quarks with special emphasis on the hadron-to-quark matter transition (through the study of finite-size effects)

and on the sudden-quark potential. Finally, Sec. V contains our conclusions.

II. TWO-QUARK NUCLEONS

The Hamiltonian for two isolated quarks moving in one dimension is given by

$$H = \frac{1}{2}P_1^2 + \frac{1}{2}P_2^2 + v(x_{12}) \\ = -\frac{1}{2}\partial_1^2 - \frac{1}{2}\partial_2^2 + \frac{1}{2}(x_1 - x_2)^2, \quad (2.1)$$

where the quark-confining potential is assumed to be harmonic and we work in units in which the quark mass, the spring constant, and \hbar are equal to 1. Throughout this paper we will also assume that quarks are fermions devoided of any intrinsic structure such as spin, flavor, and color. The ground state of the two-quark system is then given by the lowest negative-parity eigenstate of the harmonic oscillator, i.e.,

$$\psi_0(r \equiv x_1 - x_2) = r \exp(-\lambda_0 r^2/2), \quad (2.2)$$

with energy

$$\epsilon_0 = \frac{3}{\sqrt{2}} = 2.121 \quad (2.3)$$

and with

$$\lambda_0 = \frac{1}{\sqrt{2}} = 0.707, \quad (2.4)$$

being the oscillator parameter characterizing the length scale ($\lambda_0^{-1/2}$) for confinement (see Table I).

A. Many-quark potential

In extending the model to infinite quark matter, one would like to preserve certain fundamental properties that are observed in nature. For example, quarks must be confined within hadrons. This requires the presence of a confining force acting between quarks. Furthermore, the force must saturate (cluster separability); i.e., once the dynamics has dictated which quarks are to be confined within a given hadron, the residual van der Waals forces between different hadrons must vanish for large hadron separation. Finally, since quarks are identical fermions, their dynamics must be prescribed by a Hamiltonian symmetric in all quark coordinates and its behavior governed by a totally antisymmetric wave function. Clearly, a conventional many-body potential energy consisting of a sum of two-body potentials will not be able to satisfy the above requirements. If the two-body potential

falls off with increasing quark separation, it will not generate large van der Waals forces, but will neither confine. If, on the other hand, the potential confines, the force will not saturate. If the model is going to confine quarks into hadrons and, in addition, have cluster separability, the potential must be an N -body interaction that depends upon the coordinates of all N quarks. The N -body potential that we will use here was first introduced by Horowitz, Moniz, and Negele [1] as a generalization of the potential used by Lenz *et al.* [9] in the calculation of two-hadron (four-quark) scattering. The Hamiltonian for a system of N quarks is given by

$$H = T + V = -\frac{1}{2} \sum_{n=1}^N \partial_n^2 + V(x). \quad (2.5)$$

The N -body potential $V(x)$ is constructed by pairing all $N=2A$ quarks into A clusters. For a given pairing P , the pairing function $V_P(x)$ is formed by calculating the energy v (v being the confining potential) stored in the "string" connecting one quark, P_i^1 , with a second quark, P_i^2 , inside the i th hadron and then adding the contributions from all individual clusters, i.e.,

$$V_P(x) \equiv \sum_{i=1}^A v(x_{P_i^1 P_i^2}). \quad (2.6)$$

The potential energy is then chosen as the pairing function with the minimum value among all $(N-1)!!$ possible pairings of N quarks into A clusters:

$$V(x) = \min_{[P]} V_P(x). \quad (2.7)$$

The confining potential thus acts only between quarks within the same cluster. The many-body potential is therefore able to confine quarks inside hadrons, while at the same time preserving cluster separability. Although there are no long-range van der Waals forces in the model, hadrons do interact at short distances via the exchange of quarks between clusters. Furthermore, the potential is symmetric under quark exchange since the permutation of two quarks will simply cause them to exchange partners. Finally, the potential is clearly many body since moving one single quark might cause the rearrangement of all A strings. While the many-body potential is sophisticated enough to generate quark confinement, cluster separability, and the correct symmetry under quark exchange, it is conceptually quite simple. In particular, a clear picture of the quark dynamics emerges in the low- and high-density phases. In the low-density phase the dynamics favors the clustering of quarks into individual hadrons. In this phase the confinement scale is much smaller than the average interhadron separation. While the potential is essential in order to confine quarks, it is only important between quarks within the same cluster. In this phase quark exchange is suppressed and the system resembles a collection of noninteracting hadrons. In the high-density phase, on the other hand, quark exchange and string rearrangement are very prevalent. Since the length scale for quark confinement is now much bigger than the interquark separation, the potential energy becomes unimpor-

TABLE I. Energy (per quark), oscillator parameter, and mean-square radius [defined in terms of quark distances to the center of mass, i.e., $\langle r^2 \rangle = \langle \sum_i (x_i - x_{cm})^2 \rangle$] for isolated nucleons in the two- and three-quark models.

Model	E/N	λ_0	$\langle r^2 \rangle$
2Q	$3/2\sqrt{2} = 1.061$	$1/\sqrt{2} = 0.707$	$3/4\lambda_0 = 1.061$
3Q	$4/\sqrt{3} = 2.309$	$1/\sqrt{3} = 0.577$	$4/3\lambda_0 = 2.309$

tant as compared to the kinetic-energy term. In this high-density phase, then, the system behaves as a free Fermi gas of quarks. Clearly, one would like to also have a good understanding of the intermediate-density region where quarks might still be clustered inside hadrons, but where there still might be a significant amount of hadron overlap.

B. Quark pairing

Implicitly assumed in the string-flip model is the adiabatic approximation, namely, that gluons are light degrees of freedom with a dynamics that is faster in comparison to the “heavy-quark” dynamics. As a quark is moved, then, the model assumes that the gluon flux tubes adjust very rapidly to the instantaneous position of the quarks in such a way as to minimize, for example, the square of the overall length of the strings. This is the main justification to the prescription adopted in defining the many-body potential [Eq. (2.7)]. The basic problem, then, is to decide how quarks are to be paired. A flux tube leaving a quark in the system must end up on another quark. The fundamental question, however, is which quark. Presumably, lattice gauge theories solve this problem, but at a spectacular computational cost. In lattice QCD one evolves not only quarks, but also the gauge fields in accordance to the QCD dynamics. This complicated dynamics dictates the arrangement of flux tubes in the lattice. Unfortunately, unless some remarkable event develops, it is unlikely that the nuclear-matter problem will ever be solved in the lattice. One will therefore need to resort to phenomenological models. Deciding which quarks are to be paired is, nevertheless, likely to remain a general problem that most models will have to address.

Solving the quark assignment problem is probably the most taxing and challenging feature of the string-flip model. A brute force algorithm that will search among the $(2A)!/2^A A! = (N-1)!!$ possibilities ($A = N/2$ being the number of nucleons) for the two-quark nucleon case is only feasible for a very small number of nucleons. Fortunately, a power-law algorithm developed and implemented by mathematicians and economists is particularly well suited for the solution of the two-quark assignment problem [10]. The problem, however, becomes more severe for the three-quark nucleon case that will be addressed in Sec. III. Here, not only the number of possibilities, $(3A)!/6^A A!$, grows much faster with A , but more importantly, to date, there are no power-law algorithms that can solve the three-quark assignment problem. In one dimension, however, the solution to the assignment problem is trivial. Instead of searching among a factorial number of configurations, the search is limited to two configurations for the $2Q$ case and to three configurations for the $3Q$ case. For the two-quark cluster case the optimal configuration is clearly obtained by pairing quarks to their nearest neighbors. A given quark can be paired to either its nearest neighbor to the left or to its nearest neighbor to the right. Once that given pairing is selected, all remaining pairings in the lattice are fixed. For the $3Q$ case there are three possible configurations to select from since the given quark can be the leftmost,

center, or rightmost quark in the group. Even though any realistic simulation will eventually have to be carried out in three dimensions, the numerical advantages of doing one-dimensional simulations are clearly enormous. Furthermore, we expect that some qualitative features arising from the quark substructure of hadrons will remain valid in three dimensions.

C. Variational wave function

For N quarks moving in a one-dimensional box of length L , the one-parameter variational wave function is defined by

$$\Psi_\lambda(x) = e^{-\lambda V(x)} \Psi_{\text{FG}}(x), \quad (2.8)$$

where λ is the variational parameter and Ψ_{FG} is a free Fermi-gas wave function. A simple way of writing this Fermi-gas Slater determinant is achieved by adopting antiperiodic boundary conditions. This selection is simply a matter of convenience since we do not expect our results to depend significantly on the choice of boundary conditions. For this case, then, the Fermi-gas Slater determinant can be written as

$$\Psi_{\text{FG}}(x) = \prod_{n < m}^N \sin \left[\frac{\pi}{L} (x_n - x_m) \right]. \quad (2.9)$$

The Fermi-gas wave function characterizes a system of free fermions with no correlations other than those generated by the Pauli principle. The exponential term, on the other hand, characterizes the amount of clustering in the ground state through the variational parameter λ . For a dilute system of quarks, where pairs of quarks cluster into individual hadrons, the variational wave function reproduces the exact wave function of isolated clusters in the limit $\lambda \rightarrow 1/\sqrt{2}$ [see Eq. (2.4)]. In the high-density phase, on the other hand, where the interparticle separation is substantially smaller than the confinement scale, the potential becomes unimportant and the variational wave function will reproduce the Fermi-gas results in the $\lambda \rightarrow 0$ limit. Consequently, this simple one-parameter wave function is exact in the low- and high-density limits, with $\lambda^{-1/2}$ playing the role of a confinement or clustering scale. Furthermore, Horowitz, Moniz, and Negele have performed an exact evaluation of the energy per quark in one dimension using a path-integral Monte Carlo method and showed that the one-parameter variational wave function agrees extremely well with the exact results for the energy at *all* densities [1]. Establishing the reliability of the variational approach is particularly relevant for generalizations of this model to three dimensions where exact Monte Carlo solutions to fermionic systems have yet to be developed.

The analytic form of the variational wave function enables one to derive useful relations that, in particular, lead to substantial savings of computer time. For example, by performing a simple integration by parts, the expectation value of the kinetic energy,

$$\langle T \rangle_{\lambda\rho} = T_{\text{FG}}(\rho) + 2\lambda^2 \langle V \rangle_{\lambda\rho}, \quad (2.10)$$

can be written entirely in terms of the kinetic energy of a

one-dimensional free Fermi gas,

$$T_{\text{FG}}(\rho) = \pi^2 \rho^2 / 6, \quad (2.11)$$

and the expectation value of the potential energy. The kinetic energy is larger than the Fermi-gas result because of the presence of correlations induced by the clustering of quarks. Clearly, the kinetic energy is minimized in the absence of these correlations. The potential energy, on the other hand, favors a large value of lambda (small clustering length). The dynamic interplay between these two effects will generate an optimal value for the variational parameter that will minimize the total energy of the system:

$$\langle E \rangle_{\lambda\rho} = T_{\text{FG}}(\rho) + (2\lambda^2 + 1) \langle V \rangle_{\lambda\rho}. \quad (2.12)$$

Because of statistical errors in the determination of the energy, the variational parameter can be most reliably obtained by calculating zeros in the derivative of the energy with respect to lambda, i.e.,

$$\frac{d\langle E \rangle_{\lambda\rho}}{d\lambda} = 4\lambda \langle V \rangle_{\lambda\rho} - (4\lambda^2 + 2)(\langle V^2 \rangle_{\lambda\rho} - \langle V \rangle_{\lambda\rho}^2) = 0. \quad (2.13)$$

Therefore, in calculating the derivative of the energy with respect to lambda, one must evaluate not only the expectation value of the potential energy, but, in addition, also its variance. The evaluation of these expressions is simplified by the fact that most observables satisfy simple scaling relations. The only dimensionful parameters in the wave function are the clustering length $\lambda^{-1/2}$ and the size of the box L . Hence the expectation value of the potential energy can, on the basis of purely dimensional arguments, be written as

$$\langle V \rangle_{\lambda\rho} = L^2 f(\lambda L^2). \quad (2.14)$$

Instead of being a function of two independent variables, λ and $\rho = N/L$, the expectation value of the potential energy $\langle V \rangle_{\lambda\rho}/L^2$ becomes a function of a single scaling variable λL^2 . Similar relations are also satisfied by other observables. Consequently, the expectation value of these observables evaluated at a variational parameter λ_0 and density ρ_0 can now be related to the same observables evaluated at different values of λ and ρ . In particular, the expectation value of the potential energy and square of the potential energy satisfy the following scaling relations:

$$\begin{aligned} \langle V \rangle_{\lambda\rho} &= \left[\frac{\rho_0}{\rho} \right]^2 \langle V \rangle_{\lambda_0\rho_0}, \\ \langle V^2 \rangle_{\lambda\rho} &= \left[\frac{\rho_0}{\rho} \right]^4 \langle V^2 \rangle_{\lambda_0\rho_0}, \end{aligned} \quad (2.15)$$

provided the variational parameter is also scaled in the following way:

$$\lambda = \left[\frac{\rho}{\rho_0} \right]^2 \lambda_0. \quad (2.16)$$

The numerical advantages of these scaling relations

should now be evident. In general, for a given value of the variational parameter λ_0 and the density ρ_0 , the derivative of the energy with respect to λ will not vanish. However, one can now use the above relations to scale Eq. (2.13) and then search for a new value of the density that will satisfy $d\langle E \rangle_{\lambda\rho}/d\lambda = 0$. This new value of the density is given by

$$\rho = \rho_0 \left[2\lambda_0 \left[\frac{\langle V \rangle_{\lambda_0\rho_0}}{\langle V^2 \rangle_{\lambda_0\rho_0} - \langle V \rangle_{\lambda_0\rho_0}^2} - \lambda_0 \right] \right]^{-1/4}. \quad (2.17)$$

This procedure clearly leads to a substantial savings of computational effort. Instead of using several Monte Carlo runs to determine the optimal value of λ at a given density, one can now use every individual run to determine the scaled values of the variational parameter and density [Eqs. (2.16) and (2.17) respectively] at which $d\langle E \rangle_{\lambda\rho}/d\lambda$ will vanish.

III. THREE-QUARK NUCLEONS

Ultimately, the simple two-quark cluster model in one dimension will have to be generalized to three-quark nucleons moving in three dimensions. The numerical advantages of one-dimensional simulations, however, have already been mentioned in the Introduction; with the exception of one dimension, the solution of the three-quark assignment problem must rely on a brute force (factorial) algorithm. The one-dimensional model, however, can be straightforwardly generalized to three-quark nucleons. There are, at least, two reasons why the model should be generalized. First and foremost, because nature has chosen this possibility and, second, because in studying transitions between different states of matter it is important to have the composite objects also described by the correct statistics. For the two-quark cluster case, nucleons obey Bose-Einstein statistics since the totally antisymmetric quark wave function is even under the exchange of two (two-quark) nucleons.

The Hamiltonian for an isolated three-quark hadron is given as a straightforward generalization of Eq. (2.1), i.e.,

$$\begin{aligned} H &= \frac{1}{2}P_1^2 + \frac{1}{2}P_2^2 + \frac{1}{2}P_3^2 + v(x_{12}) + v(x_{23}) + v(x_{31}) \\ &= -\frac{1}{2}\partial_1^2 - \frac{1}{2}\partial_2^2 - \frac{1}{2}\partial_3^2 + \frac{1}{2}(x_1 - x_2)^2 + \frac{1}{2}(x_2 - x_3)^2 \\ &\quad + \frac{1}{2}(x_3 - x_1)^2. \end{aligned} \quad (3.1)$$

By introducing the center of mass and relative coordinates $(x_1 - x_2)$ and $[(x_1 + x_2)/2 - x_3]$ (this latter choice not being unique), the Hamiltonian separates into a free problem for the center of mass and a pair of uncoupled harmonic oscillators in the relative coordinates. The ground state of the three-quark system is then given by the lowest totally antisymmetric (in the quark coordinates) eigenstate of the above Hamiltonian, which, up to a normalization constant, is given by $(x_{ij} \equiv x_i - x_j)$

$$\psi_0(x_1, x_2, x_3) = x_{12}x_{23}x_{31} e^{-\lambda_0(x_{12}^2 + x_{23}^2 + x_{31}^2)/2}, \quad (3.2)$$

where

$$\lambda_0 = \frac{1}{\sqrt{3}} = 0.577 \quad (3.3)$$

characterizes the quark clustering length, and with

$$\epsilon_0 = 4\sqrt{3} = 6.928 \quad (3.4)$$

being the ground-state energy of the system (see Table I).

The many-body generalization of the three-quark cluster model is also straightforward. In the three-quark cluster model, one considers all possible groupings of $N=3A$ quarks into A clusters each containing three quarks. For a given grouping P , the potential energy for the i th cluster is given as the sum of pairwise harmonic interactions between quarks exactly as in Eq. (3.1), i.e.,

$$v(x_{p_i^1 p_i^2 p_i^3}) = \frac{1}{2}(x_{p_i^1} - x_{p_i^2})^2 + \frac{1}{2}(x_{p_i^2} - x_{p_i^3})^2 + \frac{1}{2}(x_{p_i^3} - x_{p_i^1})^2. \quad (3.5)$$

The total potential energy for that grouping is simply obtained by adding up the individual contributions from all A individual clusters:

$$V_P(x) \equiv \sum_{i=1}^A v(x_{p_i^1 p_i^2 p_i^3}). \quad (3.6)$$

Finally, the potential energy for the system is obtained by selecting the minimum value of the potential energy among all the $(3A)/(6^A A!)$ possible groupings:

$$V(x) = \min_{[P]} V_P(x). \quad (3.7)$$

The model is clearly symmetric in all quark coordinates and confines three quarks into individual hadrons. Although nucleons may interact via quark interchange, the force saturates at large distances and allows clusters to separate without generating large van der Waals forces.

As in the two-quark cluster case, we propose a variational approach to the calculation of ground-state observables. In fact, a one-parameter variational wave function identical in form to Eq. (2.8) is guaranteed, because of the structure of the ground-state wave function for the isolated three-quark cluster [Eq. (3.2)], to again be exact in the low- and high-density limits. Consequently, similar relations to the ones obtained in the two-quark cluster case hold in the present case as well. For example, the kinetic energy of the system is again given as a sum of a free Fermi-gas contribution plus a term generated by the presence of clustering correlations in the ground state, i.e.,

$$\langle T \rangle_{\lambda\rho} = T_{\text{FG}}(\rho) + 3\lambda^2 \langle V \rangle_{\lambda\rho}, \quad (3.8)$$

while the total energy of the system and its derivative are, respectively, given by

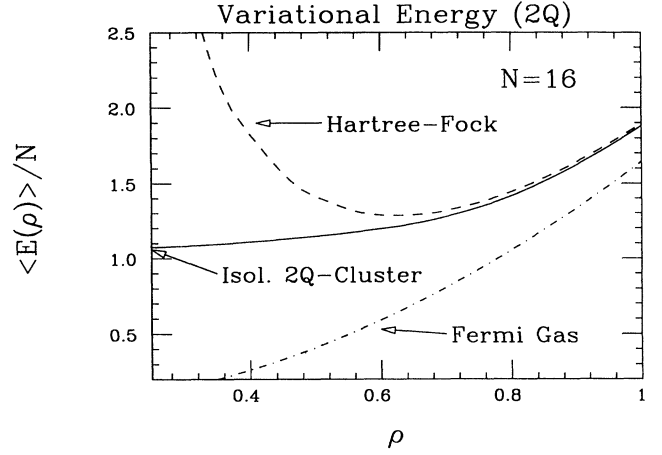


FIG. 1. Energy per quark as a function of density for the $2Q$ model. The solid line shows the results of the numerical simulations with $N=16$ quarks (statistical errors, less than 1%, are not shown). Also shown are the Hartree-Fock (dashed line) and Fermi-gas (dot-dashed line) results.

$$\langle E \rangle_{\lambda\rho} = T_{\text{FG}}(\rho) + (3\lambda^2 + 1) \langle V \rangle_{\lambda\rho},$$

$$\frac{d \langle E \rangle_{\lambda\rho}}{d\lambda} = 6\lambda \langle V \rangle_{\lambda\rho}$$

$$- (6\lambda^2 + 2) [\langle V^2 \rangle_{\lambda\rho} - \langle V \rangle_{\lambda\rho}^2]. \quad (3.10)$$

IV. RESULTS

In Fig. 1 we show the dependence of the energy per quark with density for $N=16$ quarks. The solid line is the result of the variational Monte Carlo calculation. Also shown are the free Fermi-gas (dot-dashed line) and Hartree-Fock (dashed line) results [1] (see also Table II), where

$$E_{\text{HF}}(\rho) = T_{\text{FG}}(\rho) + V_{\text{HF}}(\rho) \simeq \frac{\pi^2 \rho^2}{6} + \frac{1}{4\rho^2}. \quad (4.1)$$

The minimum in the Hartree-Fock energy separates the low-density region, where the potential energy dominates, from the kinetic-energy-dominated high-density region. The form of the potential energy in the Hartree-Fock approximation reflects both the many-body nature of the potential ($V_{\text{HF}} \sim \rho$ for two-body potential) as well as the absence of clustering correlations in the Hartree-Fock wave function. Since ground-state correlations are essential at low density, the Hartree-Fock result grossly overestimates the energy in this limit. On the other hand, the presence of strong clustering correlations in the

TABLE II. Variational vs Hartree-Fock energies in the $2Q$ model for $N=16$ quarks.

ρ	T/N	V/N	E/N	T_{HF}/N	V_{HF}/N	E_{HF}/N
0.25	0.540	0.534	1.074	0.103	3.791	3.894
0.50	0.630	0.516	1.146	0.411	0.948	1.359
0.75	0.936	0.402	1.334	0.925	0.421	1.346
1.00	1.646	0.234	1.881	1.645	0.237	1.882

variational wave function gives rise to quark confinement and to a substantial reduction in the energy as compared with the Hartree-Fock result. In this limit, then, the system resembles a free-hadron gas with an energy per quark approaching the isolated two-quark cluster limit. In the opposite (high-density) limit, the Hartree-Fock energy approaches the variational results. In this limit quarks are no longer confined inside hadrons and the system behaves as a collection of noninteracting quarks. At high density, then, there are no important correlations in the ground state beyond those generated by the Pauli principle. It is important to note that in this model nuclear matter is not bound. Even though the potential is attractive at intermediate separation (strings can flip and reduce the energy), Pauli correlations are so strong in one dimension that they preclude any possible binding between clusters.

To further emphasize the transition from hadron to quark matter, we have calculated the two-body correlation function. For an infinite system, the two-body correlation function is given by the expectation value of

$$\rho_2(r) = \frac{1}{L} \sum_{i \neq j} \delta(r - (x_i - x_j)), \quad (4.2)$$

and measures the probability of finding a quark a distance r away from another given quark. In Fig. 2 we show the results of the Monte Carlo simulations together with the two-body correlation function for an isolated cluster (dashed line) and for a free Fermi gas (solid line). The two-body correlation function for the isolated cluster is, up to normalization, given by the square of the isolated cluster wave function [Eq. (2.2)]. The free Fermi gas (normalized to one at large distances), on the other hand, is given by

$$\frac{\rho_2^{\text{FG}}(r)}{\rho_0^2} = 1 - j_0^2(k_F r), \quad k_F \equiv \pi \rho_0, \quad (4.3)$$

where ρ_0 is the one-body density and j_0 is the zeroth-order spherical Bessel function. The fact that the two-

body correlation function vanishes at the origin is simply a consequence of the Pauli principle. At low density ($\rho=0.25$) the correlation function shows a distinctive peak corresponding to the presence of the other quark inside the cluster. At intermediate separation the probability of finding another quark is exponentially suppressed [see Eq. (2.2)]. Finally, at large distances the given quark starts to feel the presence of the other quarks in the system. The peak at small distances gradually disappears with increasing density as clustering correlations cease to be important and the system approaches the free Fermi-gas phase.

In Fig. 3 we show the energy per quark and variational parameter as a function of density for several values of the number of quarks. Statistical errors for the variational parameter λ were determined in such a way that the derivative of the energy with respect to lambda at λ_{\min} (λ_{\max}) was negative (positive) within three standard deviations. The quoted value of lambda was then given as the average of λ_{\min} and λ_{\max} . It is interesting to note that while the energy per quark at small density ($\rho=0.25$) has changed by less than 1% from the isolated-cluster limit, the length scale for quark confinement ($\lambda^{-1/2}$) has increased by almost 5%. We should mention that this fact is in agreement with some explanations of the spin-independent, or old, European Muon Collaboration effect. Consistent with the above results is also the fact that at high density the variational parameter approaches zero or, equivalently, the length scale for confinement goes to infinity. In the intermediate-density region there is a rapid, although continuous, change in the variational parameter. This rapid change signals the transition from a hadron- to a quark-dominated phase.

The results that we have presented so far clearly indicate a qualitative change in the behavior of the system as the quark density is increased. These findings, however, have already been published for quite some time [1]. We have decided to include them simply for pedagogical reasons. We feel that their inclusion will give coherence to an otherwise disconnected discussion about the nature

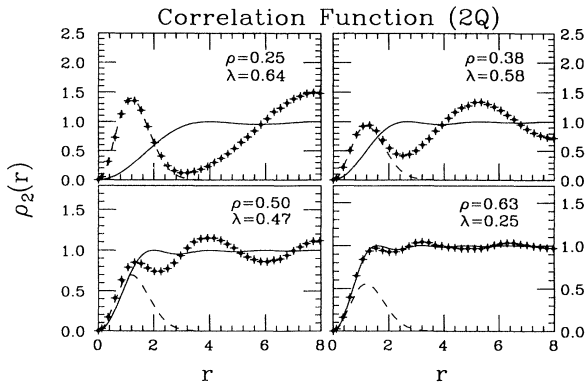


FIG. 2. Two-body correlation function for $N=16$ quarks as a function of the quark separation for various values of the density in the $2Q$ model. Also shown are the isolated two-quark cluster (dashed line) and Fermi-gas (solid line) results.

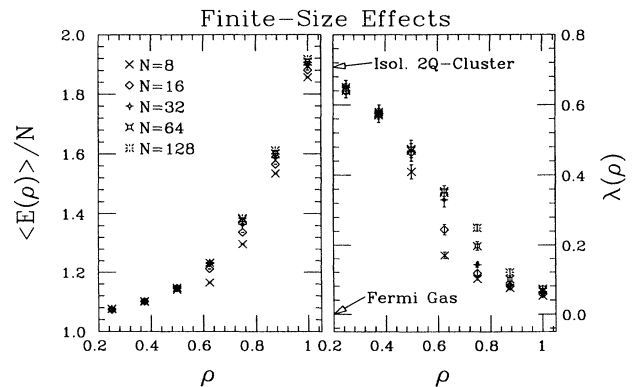


FIG. 3. Energy per quark and variational parameter λ as a function of density for various values of the number of quarks in the $2Q$ model.

TABLE III. Variational parameter λ in the $2Q$ model.

N	8	16	32	64	128
ρ					
0.250	0.650(20)	0.640(20)	0.650(20)	0.645(25)	0.640(20)
0.375	0.580(20)	0.575(15)	0.575(25)	0.570(20)	0.575(25)
0.500	0.410(20)	0.465(25)	0.470(20)	0.475(25)	0.470(30)
0.625	0.170(10)	0.245(15)	0.330(20)	0.355(15)	0.350(20)
0.750	0.101(04)	0.118(08)	0.143(08)	0.198(12)	0.250(10)
0.875	0.075(05)	0.080(10)	0.085(05)	0.100(10)	0.120(10)
1.000	0.053(02)	0.058(03)	0.060(05)	0.068(03)	0.073(08)

of the transition, which, after all, represents the ultimate goal of this work. We now proceed to discuss our new findings.

We start by examining our results as a function of the (finite) size of the system. The advent of new and more powerful computers has facilitated our task of performing numerical simulations with a large number of quarks. This fact is essential in order to estimate finite-size effects. The variational parameter λ as a function of density for several values of the number of quarks is also shown in Table III. These results, together with Fig. 3, show large finite-size effects at intermediate density. This fact gives compelling evidence in support of a transition occurring in the system at intermediate density. Irrespective of the natural length scales in the problem (all of them much smaller than the size of the box), there is evidence for a long-range coherence in the system involving the whole length of the box. One can understand these effects in terms of a balance between the “rigidity” of the quark pairings and the importance of the potential. At low density the calculations are not sensitive to finite-size effects. Although the potential energy gives a substantial contribution to the total energy of the system, the quark pairings are very rigid, making it very difficult for the strings to flip; once a quark has found a partner, it is very unlikely that it will get changed. Consequently, quarks move in a region of space comparable to the length scale for confinement and have no way of finding out that they are in fact capable of moving in a much larger space, namely,

the whole length of the box. At high density, on the other hand, string rearrangement is very prevalent. Now quarks can find out about the large size of the box because the movement of a single quark might cause the string to flip and the disturbance to propagate over the whole size of the box (note that this is strictly true only in one dimension). At high density, however, the potential energy gives only a small contribution to the total energy, and consequently we do not observe large finite-size effects. Finite-size effects are most noticeable at intermediate densities where the quark pairings are relatively loose, and so the string can occasionally flip, while at the same time the potential energy is still a substantial fraction of the total energy of the system.

Further evidence for a transition in the system is given by the response of the medium to color fields as characterized by the sudden-quark potential. The sudden-quark potential is defined as the change in the potential energy of the many-body system when two extra quarks are suddenly introduced into the system. The term sudden stems from the fact that the “slow” quarks in the system do not have time to adjust to the change brought upon them by the rapid inclusion and propagation of the two fast quarks. Consequently, the dynamical behavior of the slow quarks is described by the same variational wave function irrespective of the presence of the two extra quarks. The sudden-quark potential between two “fast” moving quarks, one located at the origin and the other one a distance r away, is then given by

$$V(r) \equiv V_{A+1}(r) - V_A,$$

$$V_{A+1}(r) = \int dx_1 \cdots dx_{2A} \Psi_\lambda^2(x_1, \dots, x_{2A}) \min_{[P]} \sum_{i=1}^{A+1} v(x_{p_i^1 p_i^2}), \quad (4.4)$$

$$V_A = \int dx_1 \cdots dx_{2A} \Psi_\lambda^2(x_1, \dots, x_{2A}) \min_{[P]} \sum_{i=1}^A v(x_{p_i^1 p_i^2}),$$

where in defining $V_{A+1}(r)$ we have assumed, in accordance with the sudden approximation, that the $N=2A$ slow moving quarks have a spatial ground-state distribution $\Psi_\lambda^2(x_1, \dots, x_{2A})$ that remains unchanged even after the introduction of the two extra quarks. The main

difference, then, between the expressions for $V_{A+1}(r)$ and V_A lies in the possibility of a new quark pairing once the two fast quarks are introduced into the system. In studying this observable we hope to understand how effective is the medium in screening the force between two color

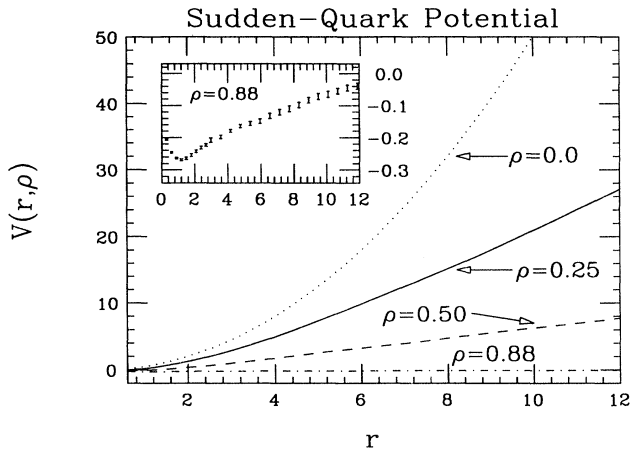


FIG. 4. Sudden-quark potential as a function of the fast-quark separation for various values of the density in the $2Q$ model. Shown in the inset is the $\rho=0.88$ result on a different energy scale. The numerical simulations were carried out with $N=32$ “slow” quarks.

charges. In the string-flip model screening happens through string rearrangement. In contrast to their interaction in free space, the two fast quarks might reduce their energy by taking advantage of the medium and pairing to nearby slow quarks. In Fig. 4 we show results for the sudden-quark potential as a function of the fast-quark separation for several values of the density. Results are shown at low ($\rho=0.25$), intermediate ($\rho=0.50$), and high density ($\rho=0.88$). Also for reference we show the zero-density result $v=r^2/2$. The potential is always attractive for very small separation. This is understood because every time the pair is introduced in a region of space occupied by a string, the string breaks, quarks recouple (one fast with one slow), and the potential energy gets reduced. The size of the attraction therefore increases with increasing density since the reduction in the potential is proportional to the amount of space occupied by all the strings. At larger separations, however, the situation is different. Although string rearrangement gives rise to screening at low and intermediate density, the sudden-quark potential will still be large (and positive) at large separations. The most interesting case happens at high density (amplified in the inset). At this density string rearrangement becomes so effective in screening the color force that even qualitative features of the potential get modified: The potential becomes always attractive and short ranged; i.e., there is perfect screening at large separations ($V \rightarrow 0$ as $r \rightarrow \infty$). Our simple model will thus predict that the formation of, for example, a J/ψ meson in relativistic heavy-ion collisions should, indeed, be strongly suppressed.

In Fig. 5 we show results for the energy per quark as a function of density for the three-quark cluster model. Qualitatively, one obtains similar results as in the two-quark cluster case: a hadron gas at low density and a free Fermi gas at high density. In fact, since Pauli correlations are even stronger in this case (see Fig. 9), they overwhelm any possible attraction coming from string

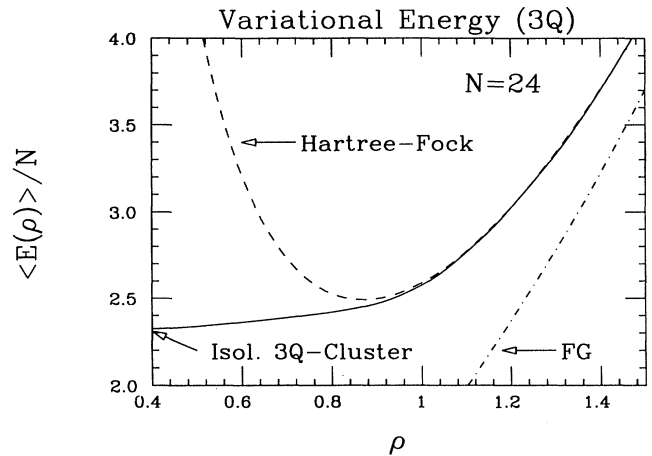


FIG. 5. Energy per quark as a function of density for the $3Q$ model. The solid line shows the results of the numerical simulations with $N=24$ quarks (statistical errors, less than 1%, are not shown). Also shown are the Hartree-Fock (dashed line) and Fermi-gas (dot-dashed line) results.

rearrangement and preclude the binding of nuclear matter. The energy per quark and the variational parameter as a function of density for several values of the number of quarks are shown in Fig. 6 (see also Table IV). Once more, there is a rapid, but smooth, variation in the intermediate-density region where the system makes the transition from hadron matter to a free Fermi gas of quarks. Some qualitative changes between the $2Q$ and $3Q$ models, however, can be seen in Fig. 7. The two-body correlation function for the isolated three-quark cluster is obtained by integrating over one of the two independent relative coordinates [see Eq. (3.2)]. At low density the correlation function still shows a distinctive peak at small distances corresponding to the presence of a nearby quark in the cluster. The presence of a third quark in the cluster, however, gives rise to an enhanced Pauli repulsion at intermediate distances, which is not seen in the $2Q$

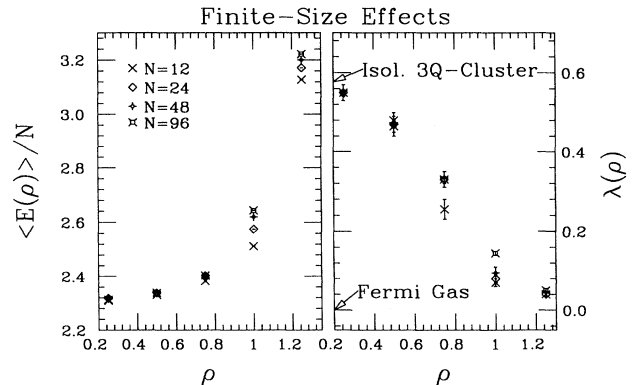


FIG. 6. Energy per quark and variational parameter λ as a function of density for various values of the number of quarks in the $3Q$ model.

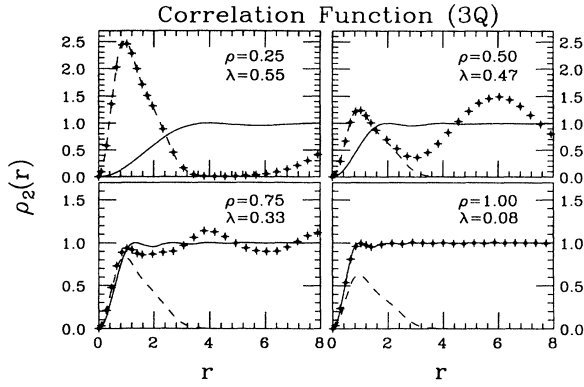


FIG. 7. Two-body correlation function for $N=24$ quarks as a function of the quark separation for various values of the density in the $3Q$ model. Also shown are the isolated three-quark cluster (dashed line) and Fermi-gas (solid line) results.

cluster case. At large enough density, however, clustering correlations are unimportant, the system behaves like a free Fermi gas of quarks, and the $2Q$ and $3Q$ models become indistinguishable.

To fully appreciate the fact that a hadron is a three-quark composite, one can calculate the three-body correlation function. For an infinite system the three-body correlation function, defined by the expectation value of

$$\rho_3(r,s) = \frac{1}{L} \sum_{i \neq j \neq k} \delta(r - (x_i - x_j)) \delta(s - (x_i - x_k)), \quad (4.5)$$

measures the probability of finding one quark a distance r away and a different quark a distance s away from yet another third given quark. For an isolated cluster the three-body correlation function is, up to normalization, simply given by the square of the isolated-cluster wave function [Eq. (3.2)]. The three-body correlation function for a free Fermi gas (normalized to one as $r, s \rightarrow \infty$) is, on the other hand, given by

$$\frac{\rho_3^{\text{FG}}(r,s)}{\rho_0^3} = 1 - [j_0^2(k_F r) + j_0^2(k_F s) + j_0^2(k_F t)] + 2[j_0(k_F r)j_0(k_F s)j_0(k_F t)], \quad (4.6)$$

where $t \equiv r - s$, and it satisfies the following properties:

$$\frac{\rho_3^{\text{FG}}(r,s)}{\rho_0^3} \xrightarrow{s \rightarrow \infty} \frac{\rho_2^{\text{FG}}(r)}{\rho_0^2} \xrightarrow{r \rightarrow \infty} 1. \quad (4.7)$$

TABLE IV. Variational parameter λ in the $3Q$ model.

N	12	24	48	96
ρ				
0.250	0.550(20)	0.550(20)	0.555(15)	0.550(20)
0.500	0.480(20)	0.470(20)	0.470(10)	0.465(25)
0.750	0.255(25)	0.330(20)	0.335(15)	0.330(20)
1.000	0.070(10)	0.080(10)	0.095(15)	0.145(05)
1.250	0.040(05)	0.040(05)	0.045(10)	0.050(05)

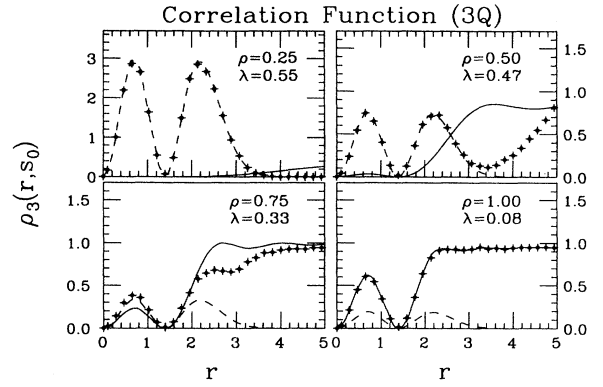


FIG. 8. Three-body correlation function for $N=24$ quarks as a function of quark separation at $s_0=1.4$ for various values of the density in the $3Q$ model. Also shown are the isolated three-quark cluster (dashed line) and Fermi-gas (solid line) results.

In Fig. 8 we show results for the three-body correlation function as a function of r for a fixed value of $s=s_0=1.4$. Essentially, it represents the probability of finding a quark at position r given the fact that two quarks are already fixed at $r=0$ and s_0 . The two nodes in the correlation function are then a consequence of the Pauli principle. The two peaks seen at low density represent the two most likely positions for the “third” quark in an isolated hadron. As the density increases, the second peak in the correlation function dissolves in much the same way as the single peak does in the two-body correlation function; hence the probability of finding the “third” quark at large distances is essentially constant. The first peak, however, remains at all densities. This is simply a consequence of having already two quarks relatively close to each other and the Pauli principle. Finally, in Fig. 9 we show the two-nucleon (NN) correlation function for the

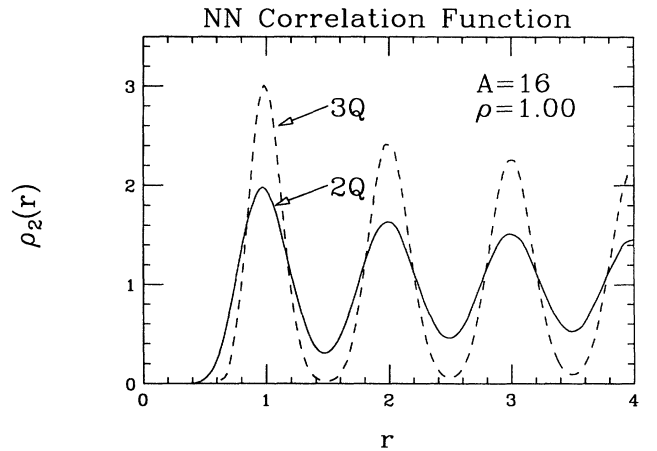


FIG. 9. Nucleon-nucleon correlation function for $A=16$ nucleons as a function of the center-of-mass separation between the quark clusters at a nuclear density of $\rho=1$. The $2Q$ model results ($N=32$ quarks) are shown in the solid line, while the $3Q$ model results ($N=48$ quarks) are given by the dashed line.

$2Q$ and $3Q$ model at a nuclear density of $\rho=1$. The single-nucleon coordinate is defined (in both models) as the center of mass of the cluster. The NN correlation function is then obtained by using Eq. (4.2), but with the distance between quark coordinates substituted with the distance between the center of mass of the clusters, i.e.,

$$\rho_2^{NN}(r) = \frac{1}{L} \sum_{i \neq j}^A \delta(r - (r_i - r_j)), \quad (4.8)$$

where r_i is the coordinate of the i th cluster,

$$r_i = \begin{cases} (x_i^1 + x_i^2)/2 & \text{for two-quark cluster,} \\ (x_i^1 + x_i^2 + x_i^3)/3 & \text{for three-quark clusters.} \end{cases} \quad (4.9)$$

The main feature displayed by the correlation function is a strong NN repulsion at short distances that is generated by the Pauli repulsion at the quark level. This relatively featureless NN correlation function displays nucleons well localized at average positions, $r=0, 1/\rho, 2/\rho, \dots$, with relatively little ‘‘Fermi motion.’’ This fact is particularly pronounced in the $3Q$ model where the Pauli principle at the quark level severely limits the motion of nucleons around their average positions.

V. CONCLUSIONS

We have calculated ground-state properties of quark matter for two- and three-quark nucleons in one dimension. We have taken full advantage of the simplicity of the quark pairing in one dimension. Ground-state properties were evaluated using a variational Monte Carlo approach to the string-flip model and studied as a function of density. Special emphasis was placed on those observables that might characterize the transition from hadron matter at low density to a free Fermi gas of quarks at high density.

The many-body nature of the potential was essential in order for quarks to cluster into hadrons and for hadrons to separate without generating large van der Waals forces. In addition, the model displayed the following limits: At low density, quarks clustered into hadrons and the system resembled a collection of weakly interacting hadrons. At high density, on the other hand, the confining potential became unimportant and the system behaved like a free Fermi gas of quarks. These results were confirmed by evaluating the equation of state for quark matter, the length scale for confinement (i.e., the variational parameter), and the two- and three-body correlation functions. In our model nuclear matter does not saturate. In fact, because of strong Pauli correlations, the system is not even bound. This, however, may be a limitation of our one-dimensional approximation and

not necessarily a limitation of the string-flip model.

The simplicity of the pairing algorithm in one dimension allowed us to carry out numerical simulations with a very large number of quarks. This fact enabled us to assess the importance of finite-size effects. We found large finite-size effects at intermediate densities. This finding made explicit the fact that a long-range coherence, typically involving the whole length of the box, was present in the system. The magnitude of the finite-size effects was attributed to a delicate balance between the ‘‘rigidity’’ of the quark pairings and the importance of the potential. Again, we argued that these large finite-size effects might depend on the one-dimensional approximation. We also tried to study the dielectric properties of the medium. We used the sudden-quark potential as an example of a generic response of the system to color fields. Color screening happened at all densities. Particularly interesting, however, were the results obtained at high density; the potential became short ranged and attractive, showing perfect screening at large fast-quark separation. We concluded that in our simple model color screening might indeed give rise to a suppression of J/ψ formation in relativistic heavy-ion collisions. Finally, we calculated the nucleon-nucleon correlation function. The main feature displayed by this observable was a strong repulsion at short distances. As in the case of most of the other observables, it was strongly dominated by the Pauli correlations at the quark level.

In summary, we have calculated ground-state properties of nuclear matter modeled directly in the quark coordinates. The dynamics in the model was generated entirely by a quark-confining potential and exchange symmetry. Although we are confident that some of the results obtained in the one-dimensional model will remain valid in three dimensions, it is clear that the model will have to be extended (three-dimensional calculations are in progress [11]). This fact is particularly true in view of the important role played by Pauli correlations in the model. Furthermore, because one of the main goals of the project is to calculate quark giant resonances, the assumption of quarks with no internal degrees of freedom will also have to be relaxed. Nevertheless, our results might be viewed as a first step in the long quest toward unambiguously identifying quark signatures in nuclei.

ACKNOWLEDGMENTS

This work was supported by the Florida State University Supercomputer Computations Research Institute, which is partially funded by the U.S. Department of Energy through Contract No. DE-FC05-85ER250000. The work at Indiana University was supported by the U.S. Department of Energy through Contract No. DE-FG02-87ER40365.

-
- [1] C. J. Horowitz, E. J. Moniz, and J. W. Negele, *Phys. Rev. D* **31**, 1689 (1985).
 [2] C. J. Horowitz, *Phys. Lett.* **162B**, 25 (1985).
 [3] P. J. S. Watson, *Nucl. Phys.* **A494**, 543 (1989).

- [4] N. Isgur, in *Proceedings of the Conference on Relativistic Dynamics and Quark-Nuclear Physics*, edited by M. B. Johnson and A. Picklesimer (Wiley, New York, 1986), p. 619.

- [5] T. Matsui and H. Satz, *Phys. Lett. B* **178**, 416 (1986); T. Matsui, *Z. Phys. C* **38**, 245 (1988).
- [6] A. Mueller, in *Proc. Seventeenth Rencontre de Moriond, Moriond, 1982*, edited by J. Tran Thanh Van (Editions Frontières, Gif-sur-Yvette, France, 1982), p. 13.
- [7] S. J. Brodsky, in *Proceedings of the Thirteenth International Symposium on Multiparticle Dynamics*, edited by W. Kittel, W. Metzger, and A. Stergiou (World Scientific, Singapore, 1982), p. 963.
- [8] I. Bergqvist *et al.*, *Nucl. Phys. A* **469**, 648 (1987); C. Ellegaard, in *Proceedings of the International Conference on Spin Observables of Nuclear Probes*, edited by C. J. Horowitz, C. D. Goodman, and G. E. Walker (Plenum, New York, 1988), p. 221.
- [9] F. Lenz, J. T. Londergan, E. J. Moniz, R. Rosenfelder, M. Stingl, and K. Yazaki, *Ann. Phys. (N.Y.)* **170**, 65 (1986).
- [10] R. E. Burkard and U. Derigs, *Lecture Notes in Economics and Mathematical Systems* (Springer-Verlag, Berlin, 1980), Vol. 184.
- [11] C. J. Horowitz and J. Piekarewicz, *Nucl. Phys. A* (to be published).